

Electron Flow in Multicenter Enzymes: Theory, Applications, and Consequences on the Natural Design of Redox Chains

Christophe Léger,^{*,†} Florence Lederer,[‡] Bruno Guigliarelli,[†] and Patrick Bertrand[†]

Contribution from the Laboratoire de Bioénergétique et Ingénierie des Protéines, UPR 9036, CNRS, IBSM and Université de Provence, 31 chemin Joseph Aiguier, 13402 Marseille Cedex 20, France, and Laboratoire d'Enzymologie et Biochimie Structurales, UPR 9063, CNRS, Avenue de la Terrasse, 91198 Gif-sur-Yvette Cedex, France

Received August 3, 2005; E-mail: christophe.leger@ibsm.cnrs-mrs.fr

Abstract: In protein film voltammetry, a redox enzyme is directly connected to an electrode; in the presence of substrate and when the driving force provided by the electrode is appropriate, a current flow reveals the steady-state turnover. We show that, in the case of a multicenter enzyme, this signal reports on the energetics and kinetics of electron transfer (ET) along the redox chain that wires the active site to the electrode, and this provides a new strategy for studying intramolecular ET. We propose a model which takes into account all the enzyme's redox microstates, and we prove it useful to interpret data for various enzymes. Several general ideas emerge from this analysis. Considering the reversibility of ET is a requirement: the usual picture, where ET is depicted as a series of irreversible steps, is oversimplified and lacks the important features that we emphasize. We give justification to the concept of apparent reduction potential on the time scale of turnover and we explain how the value of this potential relates to the thermodynamic and kinetic properties of the system. When intramolecular ET does not limit turnover, the redox chain merely mediates the driving force provided by the electrode or the soluble redox partner, whereas when intramolecular ET is slow, the enzyme behaves as if its active site had apparent redox properties which depend on the reduction potentials of the relays. This suggests an alternative to the idea that redox chains are optimized in terms of speed: evolutionary pressure may have resulted in slowing down intramolecular ET in order to tune the enzyme's "operating potential".

1. Introduction

Long-distance electron transfer (ET) is a crucial process in bioenergetics. Energy conversion via oxidative phosphorylation requires the existence of a transmembrane proton gradient, the building of which is coupled to a cascade of redox reactions.^{1,2} In the enzymes that catalyze these transformations, the electrons are transferred over distances sometimes as large as 100 Å along chains of closely spaced (<15 Å) redox relays: iron–sulfur clusters, copper centers and hemes in respiratory enzymes, or chlorophylls, pheophytins, and quinones in photosynthetic reaction centers.^{3–8}

Most of our knowledge on ET in biology comes from transient kinetics studies of reaction centers, where the large differential absorption of the porphyrin rings makes it relatively easy to detect redox processes synchronized by light flashes

and to measure their rates. These experiments are analyzed using Marcus theory,⁹ which relates the first-order rate of ET between the adjacent centers "a" and "b", the electronic coupling T_{ab} , the thermodynamic driving force $\Delta G = F(E_a^0 - E_b^0)$, and the reorganization energy λ :

$$k_{\text{ET}} \propto T_{ab}^2 \exp\left(-\frac{(\Delta G + \lambda)^2}{4\lambda RT}\right) \quad (1)$$

The magnitude and the dependence on distance of T_{ab} are modulated by superexchange,¹⁰ but it is often considered that the detailed structure of the intervening medium matters little, and the simple "ruler" proposed by Dutton and co-workers^{11,12} is sometimes used to predict the rates of intramolecular ET in cases where only the distance between the centers and their reduction potentials are known, using an arbitrary (but reasonable) value of λ .^{12,13}

Measurements of intramolecular ET rates are difficult and scarce in respiratory systems. When the ET involves a heme,

[†] Laboratoire de Bioénergétique et Ingénierie des Protéines.

[‡] Laboratoire d'Enzymologie et Biochimie Structurales.

(1) Saraste, M. *Science* **1999**, *283*, 1488–1491.

(2) Nicholls, D. G.; Ferguson, S. J. *Bioenergetic 3*; Academic Press: San Diego, 2002.

(3) Baum, R. M. *Chem. Eng. News* **1993**, *71* (Feb 22), 20–23.

(4) Stubbe, J.; Nocera, D. G.; Yee, C. S.; Chang, M. C. Y. *Chem. Rev.* **2003**, *103*, 2167–2201.

(5) Page, C. C.; Moser, C. C.; Dutton, P. L. *Curr. Opin. Chem. Biol.* **2003**, *7*, 551–556.

(6) Leys, D.; Scrutton, N. S. *Curr. Opin. Struct. Biol.* **2004**, *14*, 642–647.

(7) Gray, H. B.; Winkler, J. R. *Proc. Natl. Acad. Sci. U.S.A.* **2005**, *102*, 1534–1539.

(8) Hinchliffe, P.; Sazanov, L. A. *Science* **2005**, *309*, 771–774.

(9) Marcus, R. A.; Sutin, N. *Biochim. Biophys. Acta* **1985**, *811*, 265–322.

(10) Malak, R. A.; Gao, Z.; Wishart, J. F.; Isied, S. S. *J. Am. Chem. Soc.* **2004**, *126*, 13888–13889.

(11) Moser, C. C.; Keske, J. M.; Warncke, K.; Farid, R. S.; Dutton, P. L. *Nature* **1992**, *355*, 796–802.

(12) Page, C. C.; Moser, C. C.; Chen, X.; Dutton, P. L. *Nature* **1999**, *402*, 47–52.

(13) Unciuleac, M.; Warkentin, E.; Page, C. C.; Boll, M.; Ermiler, U. *Structure* **2004**, *12*, 2249–2256.

the transformation can still be monitored using time-resolved spectroscopy, and the enzyme-dependent strategies that have been designed to trigger the transfer include the use of temperature jumps,¹⁴ ligand photolysis,¹⁵ or reaction with photoactivated soluble reductants (such as deazaflavin, ruthenium-containing dyes, and modified cytochromes); this is informative mainly if the reaction with the soluble electron donor is fast with respect to subsequent intramolecular ET.

Iron–sulfur clusters lack the spectroscopic handles that facilitate the studies of ET to or from porphyrin rings, but NMR can be used provided $|\Delta G|$ is small and k_{ET} ranges in the kinetic window of the spectrometer.^{16–19}

Noncatalytic protein film voltammetry (PFV) has also been used to study biological ET.^{20–23} In this approach, a multicenter enzyme is adsorbed onto an electrode in such a way that ET to/from the enzyme is direct (i.e., not mediated by soluble dyes).^{24–26} Interfacial ET occurs between the electrode and the redox site that is exposed at the surface of the protein, and the electrons are transferred between this redox center and the active site, either in one step or via a chain of relays. In the case of two fumarate reductases,^{20–23} the enzyme can be adsorbed with high coverage, and the active-site flavin gives a prominent noncatalytic peak in the absence of substrate.^{27,28} In this favorable situation, when electron transfer is triggered by sweeping the electrode potential, the transient current response incorporates the delays that result from the finite rates of ET.

Using PFV, even if the electroactive coverage is too low for noncatalytic studies, a catalytic current can still be detected in the presence of substrate. Such data were obtained recently for a variety of multicenter enzymes, including mitochondrial complexes I, II, and IV,^{29–31} hydrogenases,^{32–36} copper,³⁷

heme,^{38–40} and molybdenum enzymes,^{41–45} to cite but a few. The steady-state current develops when the driving force provided by the electrode potential is high enough that the redox state of the active site is continuously regenerated following the transformation of the substrate. This signal (the “catalytic wave”) is a direct read-out of the activity of the enzyme as a function of driving force or, more precisely, as a function of the rate of reduction/oxidation of the exposed relay. In some cases, the wave is centered on the reduction potential of the active site^{34,43,46} (the change in current seems to simply reveal the formation of the redox state of the active site that is competent to transform the substrate). There are also examples where the position of the wave is closer to the reduction potential of a relay,^{31,40,44} a situation which was sometimes said to reveal rate-limiting ET to or from this mediating redox site.^{25,40,44}

However, a theoretical study is lacking to support these interpretations, as the models developed so far to interpret the catalytic data for multicenter enzymes have never described intramolecular electron transfer in a realistic manner. Most often, it was assumed that the active site is simply in redox equilibrium with^{46,47} or directly connected to the electrode.^{34,48–51} When the relays were explicitly taken into account, the assumption was made that intramolecular ET between the relay and the active site follows second-order kinetics,^{22,48,52} whereas eq 1 refers to the first-order rate constant for the reversible transition between two distinct redox states of the protein, characterized by the electrons residing on either center “a” or center “b”. The requirement that all redox (micro) states of a multicenter enzyme be considered has certainly hindered the development of more pertinent models.

Hereafter, we provide the first rigorous and fully analytical treatment of the kinetics of reversible ET in a catalytic system in the case of a minimal redox chain, consisting of a single one-electron relay connecting the electrode to a two-electron active site. We show that the precise shape and position of the catalytic wave depend not only on the redox properties of the active site but also on the thermodynamics and kinetics of ET along the entire redox chain. Conversely, such data can give

- (14) Tegoni, M.; Silvestrini, M. C.; Guigliarelli, B.; Asso, M.; Brunori, M.; Bertrand, P. *Biochemistry* **1998**, *37*, 12761–12771.
- (15) Jasaitis, A.; Rappaport, F.; Pilet, E.; Liebl, U.; Vos, M. H. *Proc. Natl. Acad. Sci. U.S.A.* **2005**, *102*, 10882–10886.
- (16) Bertini, I.; Capozzi, F.; Luchinat, C.; Messori, L.; Monnanni, R.; Scozzafava, A.; Vallini, G. *Eur. J. Biochem.* **1992**, *204*, 831–839.
- (17) Kyritsis, P.; Huber, J. G.; Quinkal, I.; Gaillard, J.; Moulis, J. M. *Biochemistry* **1997**, *36*, 7839–7846.
- (18) Kummerle, R.; Kyritsis, P.; Gaillard, J.; Moulis, J.-M. *J. Inorg. Biochem.* **2000**, *79*, 83–91.
- (19) Kummerle, R.; Gaillard, J.; Kyritsis, P.; Moulis, J.-M. *J. Biol. Inorg. Chem.* **2001**, *6*, 446–451.
- (20) Heering, H. A.; Weiner, J. H.; Armstrong, F. A. *J. Am. Chem. Soc.* **1997**, *119*, 11628–11638.
- (21) Jones, A. K.; Camba, R.; Reid, G. A.; Chapman, S. K.; Armstrong, F. A. *J. Am. Chem. Soc.* **2000**, *122*, 6494–6495.
- (22) Jeuken, L. J. C.; Jones, A. K.; Chapman, S. K.; Cecchini, G.; Armstrong, F. A. *J. Am. Chem. Soc.* **2002**, *124*, 5702–5713.
- (23) Hudson, J. M.; Heffron, K.; Kotlyar, V.; Sher, Y.; Maklashina, E.; Cecchini, G.; Armstrong, F. A. *J. Am. Chem. Soc.* **2005**, *127*, 6977–6989.
- (24) Armstrong, F. A.; Heering, H. A.; Hirst, J. *J. Chem. Soc. Rev.* **1997**, *26*, 169–179.
- (25) Léger, C.; Elliott, S. J.; Hoke, K. R.; Jeuken, L. J. C.; Jones, A. K.; Armstrong, F. A. *Biochemistry* **2003**, *42*, 8653–8662.
- (26) Armstrong, F. A. *Curr. Opin. Chem. Biol.* **2005**, *9*, 110–117.
- (27) Plichon, V.; Laviron, E. *J. Electroanal. Chem.* **1976**, *71*, 143–156.
- (28) Laviron, E. *J. Electroanal. Chem.* **1979**, *101*, 19–28.
- (29) Zu, Y.; Shannon, R. J.; Hirst, J. *J. Am. Chem. Soc.* **2003**, *125*, 6020–6021.
- (30) Hirst, J.; Sucheta, A.; Ackrell, B. A. C.; Armstrong, F. A. *J. Am. Chem. Soc.* **1996**, *118*, 5031–5038.
- (31) Haas, A. S.; Pilloud, D. L.; Reddy, K. S.; Babcock, G. T.; Moser, C. C.; Blasie, J. K.; Dutton, P. L. *J. Phys. Chem. B* **2001**, *105*, 11351–11362.
- (32) Butt, J. N.; Filipiak, M.; Hagen, W. R. *Eur. J. Biochem.* **1997**, *245*, 116–122.
- (33) Pershad, H. R.; Duff, J. L. C.; Heering, H. A.; Duin, E. C.; Albracht, S. P. J.; Armstrong, F. A. *Biochemistry* **1999**, *38*, 8992–8999.
- (34) Léger, C.; Jones, A. K.; Roseboom, W.; Albracht, S. P. J.; Armstrong, F. A. *Biochemistry* **2002**, *41*, 15736–15746.
- (35) Lamle, S. L.; Albracht, S. P. J.; Armstrong, F. A. *J. Am. Chem. Soc.* **2005**, *127*, 6595–6604.
- (36) Léger, C.; Dementin, S.; Bertrand, P.; Rousset, M.; Guigliarelli, B. *J. Am. Chem. Soc.* **2004**, *126*, 12162–12172.

- (37) Johnson, D. L.; Thompson, J. L.; Brinkmann, S. M.; Schuller, K. A.; Martin, L. L. *Biochemistry* **2003**, *42*, 10229–10237.
- (38) Angove, H. C.; Cole, J. A.; Richardson, D. J.; Butt, J. N. *J. Biol. Chem.* **2002**, *277*, 23374–23381.
- (39) Bradley, A. L.; Chobot, S. E.; Arciero, D. M.; Hooper, A. B.; Elliott, S. J. *J. Biol. Chem.* **2004**, *279*, 13297–13300.
- (40) Heering, H. A.; Wiertz, F. G. M.; Dekker, C.; de Vries, S. *J. Am. Chem. Soc.* **2004**, *126*, 11103–11112.
- (41) Aguey-Zinsou, K. F.; Bernhardt, P. V.; Leimkühler, S. *J. Am. Chem. Soc.* **2003**, *125*, 15352–15358.
- (42) Jepson, B. J. N.; Anderson, L. J.; Rubio, L. M.; Taylor, C. J.; Butler, C. S.; Flores, E.; Herrero, A.; Butt, J. N.; Richardson, D. J. *J. Biol. Chem.* **2004**, *279*, 32212–32218.
- (43) Hoke, K. R.; Cobb, N.; Armstrong, F. A.; Hille, R. *Biochemistry* **2004**, *43*, 1667–1674.
- (44) Elliott, S. J.; McElhaney, A. E.; Feng, C.; Enemark, J. H.; Armstrong, F. A. *J. Am. Chem. Soc.* **2003**, *124*, 11612–11613.
- (45) Frangioni, B.; Arnoux, P.; Sabaty, M.; Pignol, D.; Bertrand, P.; Guigliarelli, B.; Léger, C. *J. Am. Chem. Soc.* **2004**, *126*, 1328–1329.
- (46) Léger, C.; Heffron, K.; Pershad, H. R.; Maklashina, E.; Luna-Chavez, C.; Cecchini, G.; Ackrell, B. A. C.; Armstrong, F. A. *Biochemistry* **2001**, *40*, 11234–11245.
- (47) Limoges, B.; Savéant, J.-M. *J. Electroanal. Chem.* **2004**, *562*, 43–52.
- (48) Heering, H. A.; Hirst, J.; Armstrong, F. A. *J. Phys. Chem. B* **1998**, *102*, 6889–6902.
- (49) Léger, C.; Jones, A. K.; Albracht, S. P. J.; Armstrong, F. A. *J. Phys. Chem. B* **2002**, *106*, 13058–13063.
- (50) Honeychurch, M. J.; Bernhardt, P. V. *J. Phys. Chem. B* **2005**, *109*, 5766–5773.
- (51) The assumption that ET is direct is made when the Butler–Volmer formalism⁵⁵ is used to relate the rates of oxidation/reduction of the active site to the electrode potential.
- (52) See eqs 12 and B1 in ref 48, and eq 7 in ref 22.

information on the intramolecular ET kinetics, provided the reduction potentials of the centers are known. We use this model to interpret new and previously published data for various enzymes, and we provide experimental evidence that the concepts that emerge from this theoretical analysis may be generalized to multicenter enzymes comprising several electron relays. We demonstrate that, depending on how fast intramolecular ET is with respect to the active-site chemistry, the position of the catalytic wave can indeed match either the reduction potential of the relay that receives or gives electrons in the slow step or the reduction potential of the active site. In the latter case only, ET between the electrode and the active site can, indeed, be treated as direct.

Importantly, the model is not restricted to enzymes adsorbed at electrode surfaces, and we discuss the physiological implications regarding reversible ET along redox chains. We demonstrate that, when intramolecular ET is not much faster than turnover, the active site can have apparent redox properties under turnover conditions which differ from those determined at equilibrium. This may explain why evolutionary pressure has selected relays whose properties do not favor fast intramolecular ET: optimization of a redox chain may not necessarily imply acceleration of ET.

2. Experimental Methods

Samples of *Saccharomyces cerevisiae* flavocytochrome b_2 (fb2) were prepared as described in ref 53.

We used the electrochemical setup and equipment described in ref 36. The protein films were made by painting the surface of a pyrolytic graphite edge (PGE) electrode with 1 μL of 300 μM neomycin solution (Sigma) and then with 0.5 μL of stock solution of enzyme (380 μM). The buffer was a mixture of MES, HEPES, sodium acetate, TAPS, and CHES (5 mM of each component), 1 mM EDTA, and 0.1 M NaCl, titrated to pH 7 with NaOH. L-Lactate (Sigma) was added to the cell (at $T = 25^\circ\text{C}$) from a concentrated solution made in the same buffer and titrated to the appropriate pH.

As in the case of most enzymes for which PFV data are available, no reliable noncatalytic signals could be observed in the absence of substrate, and this is a direct consequence of electroactive coverage being low.²⁵

The catalytic data in Figure 2 have been recorded with the same enzyme film, and the substrate concentration was varied by injecting aliquots of a concentrated solution of L-lactate. In such experiments, the plot of activity against substrate concentration is usually easily distorted due to film loss. In contrast, the very good fit to the Michaelis–Menten equation in Figure 3A proves that the film of fb2 was perfectly stable over the time course of the experiment (despite the use of a slow scan rate) and rules out a decrease in the enzyme's activity over time resulting, for example, from a slow release of the noncovalently bound active-site flavin.

The electrode rotation rate ω was sufficiently high that raising it further produced no increase in current; thus, there was no complication due to substrate depletion near the interface or product inhibition.²⁵ The scan rate ν was small enough to achieve steady state: the shape of the baseline-subtracted signal was independent of scan direction.

All potentials are quoted against the standard hydrogen electrode (SHE).

3. Modeling

A Two-Electron Active Site Directly Wired to the Electrode. To show how the intramolecular ET kinetics affects the

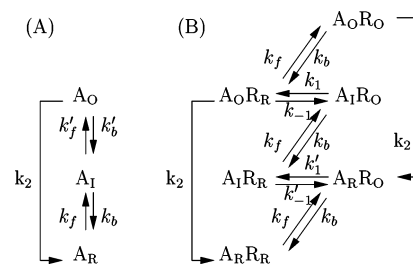


Figure 1. Catalytic schemes for a two-electron oxidation at an enzyme active site “A” directly connected to an electrode (panel A) or when a relay “R” mediates the ET between the electrode and the active site (panel B). Subscripts O, I, R, f, and b stand for oxidized, intermediate, reduced, forward, and backward, respectively.

shape of a voltammogram for a two-electron oxidation catalyzed by an adsorbed enzyme, we first recall the current equation that applies when ET occurs directly from the active site to the electrode.^{34,46} We consider that the active site exists in three redox states, termed O (oxidized), I (half-reduced intermediate), and R (reduced). As depicted in Figure 1A, the oxidized form of the active site is transformed into A_R with an apparent first-order rate constant k_2 (which incorporates the rates of substrate binding/transformation and product release). We assume that (i) the active site is fully saturated with substrate at steady state⁵⁴ (this is the case under saturating conditions, provided that binding of substrate and release of product are fast and that there is neither inhibition by nor back-reaction with the product), (ii) substrate mass transport is not limiting, and (iii) the rate of active-site oxidation as a function of electrode potential E is given by the Butler–Volmer (BV) formalism,⁵⁵ i.e., $k_b = k_0 \exp[(-f/2)(E - E_{I/R}^0)]$ and $k_f = k_0 \exp[(f/2)(E - E_{I/R}^0)]$, where $E_{I/R}^0$ is the reduction potential of the I/R couple, $f = F/RT$, and k_0 is the interfacial ET rate at zero overpotential. Analogous equations hold for k'_f and k'_b and the O/I transformation. The catalytic current i is proportional to the steady-state concentration of the oxidized state; it increases from naught at low electrode potential to a limiting value i_{lim} at high driving force according to³⁴

$$\frac{i_{\text{lim}}}{i} - 1 = u_2 + \frac{k_2}{k_0} u_{3/2} + u_1 + \frac{k_2}{k_0} u_{1/2} \quad (2a)$$

$$i_{\text{lim}} = 2FA\Gamma k_2 \quad (2b)$$

where A is the electrode surface and Γ is the electroactive coverage of enzyme. The four terms u_n are proportional to $\exp(-nfE)$ and are defined in Table 1. The terms with smaller n values contribute increasingly to the sum when the driving force increases, so that the i against E curve described by eq 2 is a sigmoidal wave which broadens at high electrode potential.

The terms u_1 and u_2 (Table 1, left) are nernstian contributions whose meaning is straightforward: a catalytic current appears when the electrode potential is high enough that the oxidized form of the active site is present.⁴⁶ The terms $u_{3/2}$ and $u_{1/2}$ reveal

(54) Taking into account substrate binding in scheme 1B is not straightforward, because this increases from 6 to 12 the number of states of the enzyme that must be considered (each state in Figure 1 should be considered free and bound to substrate).

(55) The “Marcus-like” theory of interfacial ET (ref 56) predicts how the rate of the redox process changes with the driving force $\eta = E - E^0$ for a given reorganization energy (λ). In the limiting case where $|\eta| < \lambda$, the rates of interfacial ET become independent of λ and are equally predicted by the BV formalism.

(56) Chidsey, C. E. D. *Science* **1991**, *251*, 919–922.

(53) Dubois, J.; Chapman, S. K.; Mathews, F. S.; Reid, G. A.; Lederer, F. *Biochemistry* **1990**, *29*, 6393–6400.

Table 1. Steady-State Rate Equations for a Two-Electron Catalytic Oxidation: Comparisons between the System without (Left) and with (Right) a One-Electron Relay^a

no relay	one 1-electron relay	
$i = \frac{2FA\Gamma k_2}{1+u_2+(k_2/k_0)u_{3/2}+u_1+(k_2/k_0)u_{1/2}}$	$i = \frac{2FA\Gamma k_{\text{cat}}}{1+u_2+(k_{\text{cat}}/k_0^R)u_{3/2}+u_1+(k_{\text{cat}}/k_0^R)u_x}$	$1/k_{\text{cat}} = 1/k_1 + 1/k'_1 + 1/k_2$
$u_2 = e^{-2f\left(E - \frac{-E_2}{-\frac{1}{2}(E_{\text{O}1}^0 + E_{\text{I}1\text{R}}^0)}\right)}$	$u_2 = e^{-2f\left(E - \frac{-E_2}{-\frac{1}{2}(E_{\text{O}1}^0 + E_{\text{I}1\text{R}}^0) - \Delta E_2}\right)}$	$e^{2f\Delta E_2} = 1 + k_{\text{cat}} \left(\frac{K_1 - 1}{k_1} - \frac{1}{k'_1} \right)$
$u_{3/2} = e^{-\frac{3f}{2}(E - \frac{1}{3}(2E_{\text{I}1\text{R}}^0 + E_{\text{O}1}^0))}$	$u_{3/2} = e^{-\frac{3f}{2}(E - \frac{1}{3}(2E_{\text{I}1\text{R}}^0 + E_{\text{O}1}^0))}$	
$u_1 = e^{-f\left(E - \frac{-E_1}{-E_{\text{O}1}^0}\right)}$	$u_1 = e^{-f\left(E - \frac{-E_1}{-E_{\text{O}1}^0 - \Delta E_1}\right)}$	$e^{f\Delta E_1} = 1 + k_{\text{cat}} \left[(K_1 - 1) \left(\frac{1}{k_1} + \frac{1}{k'_1} \right) + \frac{K_1}{K_1} \frac{1}{k_1} \right]$
$u_{1/2} = e^{-\frac{f}{2}(E - E_{\text{O}1}^0)} + e^{-\frac{f}{2}(E - E_{\text{I}1\text{R}}^0)}$	u_x is defined by eq. (A1) in the Appendix	

^a These equations are derived in the Supporting information.

the deviation from nernstian equilibrium which results from the steady-state competition between the reduction of the active site, with rate k_2 , and its reoxidation following interfacial ET, with a rate proportional to k_0 ,³⁴ hence, the greater k_2/k_0 , the more the steady-state concentrations of species depart from their equilibrium values, and the broader the wave.

Effect of a One-Electron Relay. We now consider the case where interfacial ET occurs between the electrode and a relay whose reduction potential is E_{R}^0 , with rates $k_{\text{b}} = k_0^{\text{R}} \exp[(-f/2)(E - E_{\text{R}}^0)]$ and $k_{\text{f}} = k_0^{\text{R}} \exp[(f/2)(E - E_{\text{R}}^0)]$. We assume that the redox state of one center has no effect on the redox properties of others; hence, a single pair of rate constants k_{f} and k_{b} describes the electron exchange between the electrode and the exposed relay, independently of the redox state of the active site. The intramolecular electron exchange between the relay and the active site is described by the rate constants k_1 , k_{-1} , k'_1 , and k'_{-1} (see Figure 1B), with $K_1 = k_1/k_{-1} = \exp[f(E_{\text{R}}^0 - E_{\text{O}1}^0)]$ and $K'_1 = k'_1/k'_{-1} = \exp[f(E_{\text{R}}^0 - E_{\text{I}1\text{R}}^0)]$. The catalytic current equates $2FAk_2$ times the steady-state concentration of the enzyme with the active site in the oxidized state; we show in the Supplementary Information that it can be written in the form

$$\frac{i_{\text{lim}}}{i} - 1 = u_2 + \frac{k_{\text{cat}}}{k_0^{\text{R}}} u_{3/2} + u_1 + \frac{k_{\text{cat}}}{k_0^{\text{R}}} u_x \quad (3a)$$

$$i_{\text{lim}} = 2FA\Gamma k_{\text{cat}} \quad (3b)$$

$$1/k_{\text{cat}} = 1/k_1 + 1/k'_1 + 1/k_2 \quad (3c)$$

At infinite driving force, i tends to a limiting value i_{lim} which incorporates irreversible intramolecular ET and catalytic transformation at the active site. The terms u_n are written in Table 1, so as to facilitate the comparison with the case where there is no relay. Instead of writing the current as a function of the seven rate constants defined in Figure 1B, it is convenient to choose as independent parameters k_{cat} , $k_{\text{cat}}/k_0^{\text{R}}$, the three reduction potentials $E_{\text{O}1}^0$, $E_{\text{I}1\text{R}}^0$, and E_{R}^0 , and the quantities ΔE_1 and ΔE_2 defined in Table 1.

It is remarkable that, despite the much greater complexity of the second kinetic scheme, the rate equation takes on essentially the same form as when there is no relay. However, some significant differences appear, as discussed below.

The terms u_1 and u_2 are no longer centered on $E_{\text{O}1}^0$ and $(E_{\text{O}1}^0 + E_{\text{I}1\text{R}}^0)/2$, respectively. When a relay is considered, E_1 and E_2 are effective reduction potentials, which are shifted away from the reduction potentials of the active site. The magnitude of

the shifts $\Delta E_1 = E_1 - E_{\text{O}1}^0$ and $\Delta E_2 = E_2 - (E_{\text{O}1}^0 + E_{\text{I}1\text{R}}^0)/2$ depends on k_{cat} and on the rate constants for intramolecular ET, and this is discussed in detail hereafter. We note already that, since $\Delta E_1 \geq 2\Delta E_2$, the presence of the relay always increases the difference $E_1 - E_2$ and thus tends to make the catalytic signal more closely resemble a one-electron wave.

The two terms that convey the competition with interfacial ET are now naturally weighted by $k_{\text{cat}}/k_0^{\text{R}}$ instead of k_2/k_0 . The term u_x is a complex function of E , but we explain in the Appendix (Supporting Information) why, in most cases, we expect it to contribute to the wave as a term $u_{1/2}$. In contrast, we have also identified some situations where this term simultaneously affects the wave shape (i.e., is large in the electrode potential range of the wave) and deviates from being proportional to $e^{(-f/2)E}$. We give in the Appendix counter-intuitive examples where the catalytic wave sharpens as the driving force increases, or where the change in activity against driving force is far from being sigmoidal; this provides a spectacular demonstration that the kinetics allowed by scheme 1B (Figure 1) can be just as complex as its mathematical treatment is straightforward. However, none of the catalytic signals reported to date illustrate these peculiar situations.

Fast Intramolecular ET. In the limiting case where the intramolecular electron transfers are much faster than k_2 (the rate of reduction of the active site), the values of ΔE_1 and ΔE_2 tend to zero,⁵⁷ the terms u_1 and u_2 are centered on $E_{\text{O}1}^0$ and $(E_{\text{O}1}^0 + E_{\text{O}1}^0)/2$, respectively, and the wave shape reports on the reduction potentials of the active site, independently of the properties of the relays which merely act as an extension of the electrode toward the active site.

Slow Intramolecular ET. The opposite limiting case occurs when the reduction of the active site is much faster than intramolecular ET. When k_2 is much greater than both k_1 and k'_1 , $1/k_{\text{cat}}$ reduces to $1/k_1 + 1/k'_1$ and the shifts ΔE_n tend to the following limits:

$$\exp(2f\Delta E_2^{\text{lim}}) = K_1 k'_1 / (k_1 + k'_1) \quad (4a)$$

$$\exp(f\Delta E_1^{\text{lim}}) = K_1 \{1 + k'_1 / [K'_1 (k_1 + k'_1)]\} \quad (4b)$$

According to eq 4a, $\exp(2f\Delta E_2^{\text{lim}}) \leq K_1$, and this sets an upper limit for the position of the two-electron wave at $E_2 \leq (E_{\text{I}1\text{R}}^0 + E_{\text{R}}^0)/2$. Likewise, the quantity $\exp(f\Delta E_1^{\text{lim}})$ is greater than K_1 ,

(57) k_{cat} reduces to k_2 and the terms ΔE_n vanish if all the following conditions apply: $k_1, k'_1 \gg k_2$; $k_1, k'_1 \gg k_2 K_1 - 1$; $k_1 \gg k_2 K_1 - 1 + K_1 / K'_1$.

which implies that the one-electron term is centered on $E_1 \geq E_R^0$.

General Case. In the most general situation, the values of E_1 and E_2 depend on k_2 and on the intramolecular ET rate constants, and it is convenient to write the shifts in the form

$$\Delta E_2 = (2f)^{-1} \ln(1 + [\exp(2f\Delta E_2^{\text{lim}}) - 1]k_{\text{cat}}/k_i) \quad (5a)$$

$$\Delta E_1 = f^{-1} \ln(1 + [\exp(f\Delta E_1^{\text{lim}}) - 1]k_{\text{cat}}/k_i) \quad (5b)$$

where $1/k_i = 1/k_1 + 1/k'_1$, $1/k_{\text{cat}} = 1/k_2 + 1/k_i$, and ΔE_n^{lim} are defined by eqs 4. Equations 5 show that the shifts vary in a monotonic way from $\Delta E_n = 0$ when intramolecular ET is fast ($k_i \gg k_{\text{cat}}$) to $\Delta E_n = \Delta E_n^{\text{lim}}$ when it is rate limiting ($k_i = k_{\text{cat}}$), and this is why the position of the wave can give quantitative information on the kinetics of intramolecular ET, as illustrated hereafter.

4. Applications

Fast Intramolecular ET. The literature provides several examples that illustrate the limiting case of fast intramolecular ET. For example, in *Allochromatium vinosum* NiFe hydrogenase, the electrons are mediated by a linear chain consisting of three FeS clusters, and the electrochemical data for proton reduction could be modeled assuming that direct ET occurs between the electrode and the active site,³⁴ the oxidation and reduction of which follows Butler–Volmer kinetics. Our model shows that this is not in contradiction with the electron being transferred by hopping between adjacent centers.

The oxidation of succinate by *Escherichia coli* fumarate reductase,⁴⁶ which contains an active-site flavin wired by three FeS clusters,²³ exemplifies the case where k_2 is so small (the enzyme is actually tuned to operate in the reverse direction) that the active site is in redox equilibrium with the electrode potential.

In both cases, intramolecular ET is so fast that it does not affect the dependence of activity on driving force. Thus, the electrochemical data can be used to gain insights into the chemistry that occurs at the active site, but they hold no information on the kinetics of intramolecular ET.

Intramolecular ET in Flavocytochrome b_2 . In flavocytochrome b_2 (fb2),⁵⁸ the electrons produced upon oxidation of L-lactate at the FMN active site are transferred to the redox partner via a single heme. When adsorbed onto a PGE electrode, this enzyme displays catalytic activity, as shown in Figure 2.

At high electrode potential, we observe a residual slope in the voltammogram, whereas eqs 2 and 3 predict a plateau. This has been observed for many enzymes and explained on the basis of disorder among the adsorbed enzyme molecules, resulting in a dispersion of interfacial ET rate constants.^{25,49} Thus, the method proposed in ref 49 was used to analyze the voltammograms, and eq S14 (Supporting information) was used instead of eq 3 to fit the data. As discussed previously, this changes neither the number nor the qualitative meaning of the parameters that need to be adjusted; the main difference is that a quantity proportional to i_{lim} (termed $i_{\text{lim}}/\beta d_0$) is adjusted in place of the true limiting current, which is not reached in the experimental range of electrode potential. The procedure used

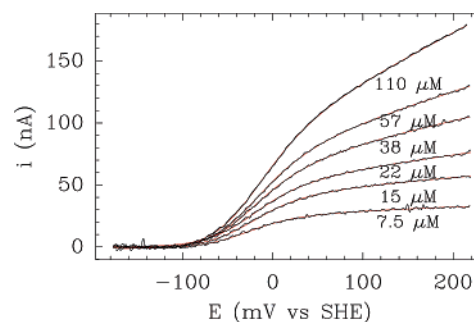


Figure 2. Substrate concentration dependence of catalytic voltammograms for lactate oxidation by flavocytochrome b_2 (black lines), and fits to eq S14 (red lines). Equation S14 is given in the Supporting Information; it is equivalent to eq 3 after the dispersion of k_0^R values is accounted for.⁴⁹ The data have been corrected only by subtracting a voltammogram recorded in the absence of substrate. $T = 25$ °C, pH 7, $\omega = 1000$ rpm, $\nu = 5$ mV/s, lactate concentration as indicated.

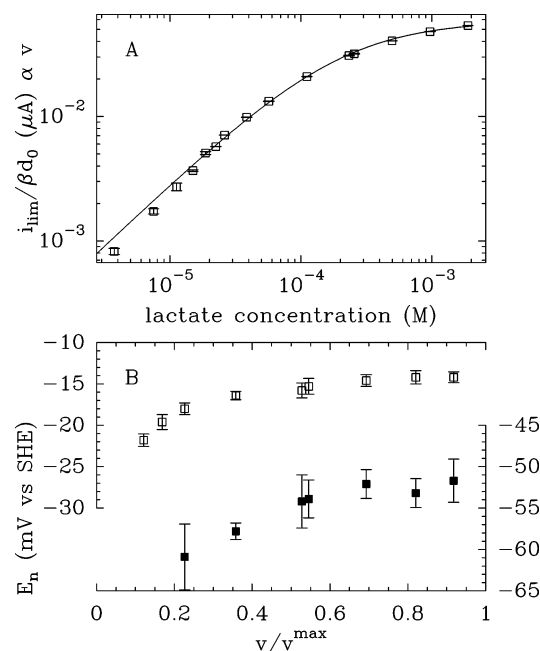


Figure 3. Result of the fits of voltammograms for lactate oxidation to eq S14 (Supporting Information). Panel A: The change in $i_{\text{lim}}/\beta d_0$ against lactate concentration is fit to the Michaelis–Menten equation. Panel B: Values of E_1 (□ and left axis) and E_2 (■ and right axis) plotted against v/v^{max} . Error bars show the difference between the parameters determined for scanning in the oxidative and reductive directions.

to analyze the data is explained in detail in the Supporting Information.

The best fits of the voltammograms overlay perfectly the data in Figure 2; no systematic deviation was observed. The adjusted value of $i_{\text{lim}}/\beta d_0$ is proportional to the turnover rate ν , and its dependence on substrate concentration can be fit to measure the Michaelis constant^{25,43,49} and a quantity proportional to ν^{max} (Figure 3A). We found $K_m = 200$ μM (in solution assays,⁵⁹ the K_m value for lactate oxidation depends on the electron acceptor, ionic strength, and temperature, and it ranges from 240 to 600 μM). Figure 3B shows the best values of E_1 and E_2 plotted as a function of v/v^{max} .

Intramolecular ET in fb2 has been previously characterized by performing redox titrations and temperature jump experi-

(58) Lederer, F. Flavocytochrome b_2 . *Chemistry and Biochemistry of Flavoenzymes*; CRC Press: Boca Raton, FL, 1991; pp 153–241.

(59) Rouvière, N.; Mayer, M.; Tegoni, M.; Capeillère-Blandin, C.; Lederer, F. *Biochemistry* **1997**, *36*, 7126–7135.

ments.¹⁴ At pH 7, $E_{O/I}^0 = -45$ mV, $E_{I/R}^0 = -135$ mV, and $E_R^0 = -3$ mV. The rate k_1' of ET from reduced FMN to heme is much faster than k_1 from semiquinone to heme (thus, $k_i \approx k_1$) and $K_1' \gg 1$. Equations 4 give $\exp(f\Delta E_1^{\text{lim}}) = \exp(2f\Delta E_2^{\text{lim}}) = K_1$; thus, $E_1^{\text{lim}} = E_R^0 = -3$ mV and $E_2^{\text{lim}} = (E_R^0 + E_{I/R}^0)/2 = -69$ mV. Therefore, E_1 and E_2 should range in the intervals $[E_{O/I}^0, E_R^0]$ and $[(E_{O/I}^0 + E_{I/R}^0)/2, (E_R^0 + E_{I/R}^0)/2]$, respectively, the exact value depending on how fast k_2 is with respect to intramolecular ET.

In Figure 3B, the values of $E_1 = -15$ mV and $E_2 = -53$ mV under saturating conditions are close to the values $E_1^{\text{lim}} = -3$ mV and $E_2^{\text{lim}} = -69$ mV. According to eqs 5, this implies that intramolecular ET is not very fast with respect to k_{cat} . Indeed, $k_{\text{cat}} \approx 270$ s⁻¹ at 30 °C from ref 59, while values of k_1 were found in the range 80–500 s⁻¹, depending on experimental conditions (buffer composition and temperature).¹⁴ This is also consistent with the isotope effect under steady-state conditions being significant but smaller than that for flavin reduction, measured using stopped flow.⁵⁹

Although the model cannot predict accurately the change in E_n against substrate concentration because it does not explicitly consider the steps for substrate binding, the trends seen in Figure 3B are qualitatively consistent with eqs 5: both E_1 and E_2 increase with increasing turnover rate, and this is expected because E_R^0 is slightly more positive than $E_{O/I}^0$.

This is our first illustration that, under turnover conditions, the apparent redox properties of an enzyme depend not only on the reduction potential of the active site but also on the thermodynamics and kinetics of intramolecular ET.

Intramolecular ET in Sulfite Oxidase. In chicken liver sulfite oxidase,⁶⁰ the molybdenum active site passes on electrons to cytochrome *c* via a small heme domain that is tethered to the molybdenum domain by a flexible loop. The values of $E_{O/I}^0$ and $E_{I/R}^0$ (for Mo(VI)/(V) and Mo(V)/(IV), respectively), interpolated at pH 8 from the data in Table 1 of ref 61, are ~ 0 mV and ~ -200 mV, respectively. When the enzyme is adsorbed onto an electrode, a one-electron noncatalytic peak at $E_R^0 = +90$ mV, pH 8, reveals the reduction potential of the heme (see Figure 1 in ref 44); under saturating concentrations of substrate, a one-electron catalytic wave is observed whose position ($E_1 = +65$ mV at pH 8, 20 °C) is shifted from $E_{O/I}^0$ and shows little dependence on pH (Figure 2 in ref 44); this contrasts with what is observed for the reduction potentials of the molybdenum couples (Table 1 in ref 61). These observations were said to reveal rate-limiting ET from Mo to heme.^{25,44} In contrast, other authors have interpreted the results of kinetic studies of the same enzyme assuming that intramolecular ET was rapid.⁶² We will now show how our model can be used to gain more quantitative information in this respect.

From the values of the reduction potentials above, $K_1' \gg 1$; in eq 4b this sets $\Delta E_1^{\text{lim}} = f^{-1} \ln K_1 = E_R^0 - E_{O/I}^0 = 90$ mV. Using the value of $\Delta E_1 = E_1 - E_{O/I}^0 = 65$ mV in eq 5b gives $k_1/k_{\text{cat}} = 2.9$ (this ranges from 2.7 to 4.8, depending on the exact value of $E_{O/I}^0$ in the interval $[-60$ mV, $+60$ mV]). This shows that intramolecular ET is neither very fast nor fully rate-

limiting: the rates of ET from Mo to heme and of chemical transformation at the active site must be of the same order of magnitude.

Using the value of $k_{\text{cat}} = 95$ s⁻¹ determined under saturating concentrations of sulfite and oxidized cytochrome *c*, at pH 8, 25 °C (ref 62), we determine $k_i = k_1 k_1' / (k_1 + k_1')$ in the range 250–450 s⁻¹. Since the driving force for k_1' (ET from Mo^{IV} to oxidized heme) is much larger than that for k_1 (from Mo^V to heme), we expect $k_1' \gg k_1$, and thus $k_i \approx k_1 \approx 250$ –450 s⁻¹. This can be compared to $k_{\text{ET}} = k_1 + k_{-1} = 800$ s⁻¹, determined at pH 8 using flash photolysis on the same enzyme (see Table 1 in ref 63).⁶⁴

It should be emphasized that we estimated the efficacy of intramolecular ET from data obtained with the enzyme sulfite oxidase affixed to an electrode surface, most likely by the heme domain.⁴⁴ This adsorption may hinder the domain–domain motion that plays an important role in the ET process,⁶⁵ and this could make ET slower than when the enzyme is free in a dilute, uncrowded⁶⁶ solution.

Interprotein ET. The complex between complex IV and cytochrome *c* adsorbed on a modified Au electrode³¹ is an example where the catalytic process leading to the reduction of O₂ is limited by interprotein ET, and, as discussed in ref 25, this is apparent from the position of the catalytic wave, which is centered on the reduction potential of the cytochrome (Figure 8 in ref 31).

An Artificial Wire. The model we propose also applies to man-made, one-dimensional redox chains linking electrodes to enzymes. For example, in ref 67, Willner and co-workers report on the reconstitution of apo-glucose oxidase (Gox) on a FAD cofactor linked to a pyrroquinoline quinone (PQQ) phenylboronic acid monolayer self-assembled on a gold electrode. Fast interfacial ET to/from the PQQ moiety is observed. The position of the catalytic wave for glucose oxidation shows little dependence on substrate concentration (Figure 4 in ref 67) and is centered slightly above the reduction potential of the PQQ ($E_R^0 = 110$ mV vs SHE at pH 7, from Figure 2 in ref 67; this is much greater than the reduction potential of the FAD in Gox,⁶⁸ $E_{O/I}^0 = -60$ mV at pH 5.3), which we now interpret in terms of ET from FAD to PQQ being rate-limiting during turnover. That PQQ is a two-electron relay prevents further analysis of these data with the model we developed.

5. Discussion

The kinetics of ET along redox chains in multicenter enzymes is very often thought of as a series of irreversible steps.⁶⁹ This is certainly a good approximation in reaction centers, where backward electron transfers and charge recombinations are avoided. However, the substrates of respiratory enzymes often

(63) Sullivan, E. P.; Hazzard, J. T.; Tollin, G.; Enemark, J. H. *Biochemistry* **1993**, *32*, 12465–12470.

(64) In ref 63, the experimental temperature is not stated, and as the authors point out, the determined value of $K_1 = k_1/k_{-1}$ is not consistent with the reduction potentials of the centers. This prevented us from determining k_1 and k_{-1} from the values of k_{ET} and K_1 .

(65) Feng, C.; Kedia, R. V.; Hazzard, J. T.; Hurley, J. K.; Tollin, G.; Enemark, J. H. *Biochemistry* **2002**, *41*, 5816–5821.

(66) Ellis, R. J. *Trends Biochem. Sci.* **2001**, *26*, 597–604.

(67) Zayats, M.; Katz, E.; Willner, I. *J. Am. Chem. Soc.* **2002**, *124*, 14724–14735.

(68) Stankovich, M.; Massey, L. S. V. *J. Biol. Chem.* **1978**, *253*, 4971–4979.

(69) The assumption that intramolecular ET is irreversible is made when the overall rate of ET through a chain is estimated by summing the reciprocals of the rates calculated or measured for the successive ET steps. For example, see the calculations related to the heme chain of the cytochrome of *Rhodospseudomonas viridis*, Figure 2 in ref 12.

(60) Kisker, C.; Schindelin, H.; Pacheco, A.; Wehbi, W. A.; Garrett, R. M.; Rajagopalan, K. V.; Enemark, J. H.; Rees, D. C. *Cell* **1997**, *91*, 973–983.

(61) Spence, J. T.; Kipke, C. A.; Enemark, J. H.; Sundespen, R. A. *Inorg. Chem.* **1991**, *30*, 3011–3015.

(62) Brody, M. S.; Hille, R. *Biochemistry* **1999**, *38*, 6668–6677.

provide only moderate driving forces,⁷⁰ and neglecting the reverse reactions leads to an oversimplified picture of the ET kinetics which lacks the important features that we discuss here.

The technique called protein film voltammetry (PFV)^{24–26} makes the driving force a natural experimental parameter: when a multicenter redox enzyme is adsorbed onto an electrode, in the presence of substrate, the activity of the enzyme is measured as a current as a function of the electrode potential, which affects the rate of oxidation and reduction of the redox relay that is exposed at the surface of the protein. Every point along the voltammogram is an initial rate for a given driving force, and we have shown how the entire shape of the catalytic wave relates to both the active-site chemistry and intramolecular ET.

We have considered the case where a single relay connects the active site to the electrode (Figure 1B). At infinite driving force (high potential for a catalytic oxidation), the steady-state concentration of enzyme in which the relay is reduced tends to zero and the activity depends only on the rates of forward ET; in this case only, the kinetics is adequately described by a succession of independent, irreversible steps:

$$\frac{1}{k_{\text{cat}}} = \frac{1}{k_1} + \frac{1}{k'_1} + \frac{1}{k_2} \quad (6)$$

Therefore, the magnitude of the wave, which is proportional to k_{cat} , does not depend on the rates of backward ET and contains no information on the energetics of the ET chain. In contrast, at moderate (and thus physiological) driving force, forward and backward transitions between all the enzyme's redox microstates must be considered, the turnover rate is necessarily lower than that predicted by eq 6, and the position and shape of the voltammogram hold the information about intramolecular ET.

We have shown on several examples that PFV can be used to diagnose slow intramolecular ET: for a catalytic oxidation, this results in a broad ($n = 1$) wave, centered close to the reduction potential of the relay that accepts the electrons in the slow step ($E_1 \geq E_{\text{R}}^0$), and the position of the wave is expected to show little dependence on the experimental parameters that may affect the reduction potential of the active site alone (e.g. the concentrations of substrate, product, and inhibitor, and possibly the pH): our model supports the concept of “control center” introduced in ref 25, and gives it theoretical grounds.

It is remarkable that schemes 1A and 1B (Figure 1) lead to rate equations that take on essentially the same form (eq 3 is similar to eq 2, since we showed in the Appendix that, in most cases, the term u_x behaves like $u_{1/2}$). Therefore, regarding the fit of the PFV data, considering direct or mediated ET does not change the number of parameters that have to be adjusted. However, this changes the physical meaning of these parameters: when ET is mediated by a relay, the position and shape of the catalytic wave depend on *apparent* reduction potentials, E_1 and E_2 , which can depart from the reduction potentials of the active site.⁷¹ These shifts occur when intramolecular ET is not fast enough to compete successfully with the reaction of the active site with substrate. The values of E_1 and/or E_2 can be measured by fitting the catalytic wave shapes, and the

comparison with the true reduction potentials of the active site can be used to gain information about the ET kinetics: the method was illustrated by discussing data obtained with flavocytochrome b_2 and sulfite oxidase.

So far, we have considered the cases where the enzyme gives electrons to an electrode, but our main conclusions also apply when a soluble redox partner accepts the electrons. In the latter case, Marcus theory,⁵⁶ rather than Butler–Volmer theory, should be used to describe the rate constants k_f and k_b in Figure 1B. However, provided the driving force is small, eq 1 reads

$$k_{\text{ET}} \propto T_{\text{ab}}^2 \exp\left(-\frac{\lambda}{4RT}\right) \exp\left(\pm \frac{\Delta G}{2RT}\right) \quad (7)$$

That is, the dependence of k_{ET} on driving force is the same as that predicted by the BV formalism for interfacial ET, which applies when $|E - E_{\text{R}}^0| < \lambda$ (ref 55):

$$k_{\text{ET}} = k_0^{\text{R}} \exp\left(\pm \frac{F}{2RT}(E - E_{\text{R}}^0)\right) \quad (8)$$

This shows that, in PFV experiments, the overpotential $F(E - E_{\text{R}}^0)$ has the same meaning as the driving force $\Delta G = E_{\text{partner}}^0 - E_{\text{R}}^0$ in more traditional (homogeneous) kinetics.^{42,73}

Regarding biological ET, we have shown that the usual picture, where the kinetics is represented as a series of irreversible steps, is oversimplified. When reversibility is considered, the thermodynamics and kinetics of the entire redox chain (including the active site) must be taken into account, and this gives an integrated picture of the ET dynamics, where the behavior of the enzyme as a whole depends on every relay. Two cases are naturally distinguished on the basis of how fast intramolecular ET is with respect to the chemical transformation at the active site. When intramolecular ET does not limit turnover, everything happens as if electrons were transferred directly between the redox partner and the active site, and the only effect of the redox chain is to transmit the driving force across the enzyme. In contrast, if intramolecular ET is not very fast with respect to turnover, the driving force that is required to trigger catalysis depends on both the reduction potentials of the relays and the kinetics of intramolecular ET: under turnover conditions, everything happens as if the active site had redox properties that are controlled, or tuned, by the ET chain.

There has been a considerable debate regarding whether the redox chains in multicenter enzymes have been optimized to increase the rates of intramolecular ET.^{7,12} This was questioned by the numerous examples where electrons do not simply flow toward relays of increasing reduction potentials and statistical studies did not detect the higher packing density of the protein in the region between the centers, which would have led to an enhancement of ET.^{5,12} Our work gives an alternative point of view, according to which optimization of the ET chain need not be considered in terms of speed: the properties of the relays, and therefore the ET kinetics, may well have been optimized, in some cases, to tune the apparent reduction potential of the active site. There can be no such effect in a particular enzyme (and no evolutionary pressure)⁵ if the rate of ET is much faster than

(70) Osyczka, A.; Moser, C. C.; Daldal, F.; Dutton, P. L. *Nature* **2004**, *427*, 607–612.

(71) This is reminiscent of a common situation in enzyme kinetics. For example, very complex kinetic models lead to the Michaelis–Menten rate equation, which is a function of only two independent parameters (K_m and k_{cat}), and the Michaelis constant is only an apparent dissociation constant.⁷²

(72) Cornish-Bowden, A. *Fundamentals of Enzyme Kinetics*, 3rd ed.; Portland Press: London, 2004.

(73) Elliott, S. J.; Léger, C.; Pershad, H. R.; Hirst, J.; Heffron, K.; Blasco, F.; Rothery, R.; Weiner, J.; Armstrong, F. A. *Biochim. Biophys. Acta* **2002**, *1555*, 54–59.

turnover, but in contrast to reaction centers where charges must be separated on the microsecond time scale, very fast ET is not a requirement in respiratory systems.

Acknowledgment. We thank Alexander Kuhn (University of Bordeaux I, France) and Wolfgang Nitschke (CNRS, Marseilles) for fruitful discussions. This work was supported by the CNRS, the University of Provence, and the City of Marseilles.

Supporting Information Available: The Appendix, derivations of eqs 2 and 3, figure showing the raw data for lactate oxidation by fb2, and description of the procedure used to fit these data. This material is available free of charge via the Internet at <http://pubs.acs.org>.

JA055275Z